

The Microphthalmia-associated transcription factor is involved in gastrointestinal stromal tumor growth

Elizabeth Proaño-Pérez ^{1,2,3}, Eva Serrano-Candelas ^{1,2}, Alfonso García-Valverde ⁴, Jordi Rosell ⁴, David Gómez-Peregrina ⁴, Arnau Navinés-Ferrer ^{1,2}, Mario Guerrero ¹, César Serrano ^{4,5}, Margarita Martín ^{1,2}

¹ Biochemistry and Molecular Biology Unit, Biomedicine Department, Faculty of Medicine and Health Sciences, University of Barcelona, Barcelona, Spain

² Clinical and Experimental Respiratory Immunoallergy (IRCE), Institut d'Investigacions Biomediques August Pi i Sunyer (IDIBAPS), Barcelona, Spain

³ Faculty of Health Sciences, Technical University of Ambato, Ambato-Ecuador

⁴ Sarcoma Translational Research Program, Vall d'Hebron Institute of Oncology (VHIO), Hospital Universitario Vall d'Hebron, Vall d'Hebron Barcelona Hospital Campus, C/ Natzaret, 115-117, 08035, Barcelona, Spain.

⁵ Department of Medical Oncology, Vall d'Hebron University Hospital, Barcelona, Spain.

CORRESPONDENCE:

M. Martín, Biochemistry Unit, Biomedicine Department, Faculty of Medicine, University of Barcelona, Carrer de Casanova 143, E-08036 Barcelona, Spain. E-mail address: martin_andorra@ub.edu. Phone: (34) 93-4024541. Fax: (34) 93-4035882.

RUNNING TITLE

MITF in GIST cell survival

Keywords:

MITF / Cell survival / Cell cycle / Gastrointestinal stromal tumors (GIST)

ABSTRACT

Gastrointestinal stromal tumors (GISTs) are the most common neoplasms of mesenchymal origin, and most of them emerge due to the oncogenic activation of KIT or PDGFRA receptors. Despite their relevance in GIST oncogenesis, critical intermediates mediating the KIT/PDGFRA transforming program remain mostly unknown. Previously, we found that the adaptor molecule SH3BP2 was involved in GIST cell survival, likely due to the co-regulation of the expression of KIT and Microphthalmia-associated transcription factor (MITF). Remarkably, MITF reconstitution restored KIT expression levels in SH3BP2 silenced cells and restored cell viability. This study aimed to analyze MITF as a novel driver of KIT transforming program in GIST. Firstly, MITF isoforms were characterized in GIST cell lines and GIST patients' samples. MITF silencing decreases cell viability and increases apoptosis in GIST cell lines irrespective of the type of KIT primary or secondary mutation. Additionally, MITF silencing leads to cell cycle arrest and impaired tumor growth *in vivo*. Interestingly, MITF silencing also affects ETV1 expression, a lineage survival factor in GIST that promotes tumorigenesis and is directly regulated by KIT signaling. Altogether, these results point to MITF as a key target of KIT/PDGFRA oncogenic signaling for GIST survival and tumor growth.

1. INTRODUCTION

Gastrointestinal stromal tumors (GISTs) are the most common neoplasms of mesenchymal origin ¹, and arise from the interstitial cells of Cajal (ICCs), located in the submucosal and myenteric plexus of the gastrointestinal tract ². GIST pathogenesis is defined by mutually exclusive gain-of-function mutations in *KIT* or platelet-derived growth factor receptor α (*PDGFRA*) genes (75% and 10% of cases, respectively), which constitutively activate KIT and PDGFRA oncoproteins. As these receptors play a crucial role in cell survival, proliferation, and differentiation, activating mutations are thought to be the initiating events conferring an oncogenic capacity to proliferate and form tumors ³. Given the relevance of KIT and PDGFRA receptor tyrosine kinases in GIST survival, targeted inhibition of these receptors with first-line imatinib provides substantial clinical benefit in metastatic GIST patients ⁴. Remarkably, KIT/PDGFRA oncogenic signaling remains essential at the time of imatinib progression, as resistance is largely driven by the polyclonal emergence of KIT secondary mutations ³.

Previously, our group described that the cytoplasmic adaptor molecule SH3-binding protein 2 (SH3BP2) regulates the expression and signaling of KIT receptor tyrosine kinase in both mast ⁵ and GIST cell models ⁶. Silencing of SH3BP2 impairs KIT expression and promotes cellular apoptosis. Furthermore, SH3BP2 regulates not only KIT at the transcriptional level, but also the expression of microphthalmia-associated transcription factor (MITF) at the post-transcriptional level ⁵. Accordingly, MITF overexpression in SH3BP2 silenced cells significantly reverts cellular apoptosis in GIST cell lines ⁶.

MITF is a basic helix-loop-helix leucine zipper (bHLH-Zip), a dimeric transcription factor involved in the generation and function of mast cells ⁷, melanocytes ⁸, osteoclasts ^{9,10}, and retinal pigmented epithelium ¹¹. Mutations in *MITF* lead to defects in melanocytes, the retinal pigmented epithelium, mast cells, and osteoclasts ¹². Although MITF has been extensively studied in melanoma ¹²⁻¹⁵ its potential role in GIST biology remains unknown.

Due to alternative promoter usage and splicing, the human MITF gene generates multiple mRNAs and protein isoforms, which differ primarily at their 5'-ends and

amino termini, respectively ¹⁶. MITF isoforms share the carboxyl portion, including the transcriptional activation domain, the bHLH-Zip structure required for transcription, and DNA binding/dimer ¹⁷. MITF-A and MITF-C isoforms are widely expressed in many human tissues and have the highest expression levels compared with other MITF isoforms ¹⁵. The MITF-M isoform is found mainly in the skin, adipose tissue, muscle, uterus ¹⁶, and kidney ¹⁸, and it was identified as an oncogene in melanoma ^{19–21}. MITF-M high and MITF-M low expression can be seen in melanoma tumors ^{22–24}. This apparent contradiction is supported by the fact that high MITF-M expression is associated with a differentiated and proliferative phenotype, whereas low MITF-M expression is attributed to a dedifferentiated, invasive, apoptosis-resistant, and melanoma-initiating cell phenotype. Differential expression of MITF could be due to a reversible phenotypic switch linked to melanoma plasticity and intratumor heterogeneity ^{25,26}.

The most prominent transcription factor involved in the ICC-GIST-specific transcription network is ETV1, which belongs to the ETS family of transcription factors. ETV1 is regulated by KIT, which lengthens ETV1 protein stability by MAP kinase signaling downstream of oncogenic KIT signaling ²⁷. ETV1 directly and positively regulates KIT expression, generating a positive feedback track to promote tumorigenesis ²⁸. Interestingly, a mechanistic relationship between ETV1 and MITF in melanocytes has been demonstrated (Jané-valbuena *et al.*, 2011).

Lately, the forkhead family member FOXF1 was found to regulate the transcription of KIT and ETV1 ²⁹ directly. FOXF1 works upstream of ETV1, providing chromatin accessibility, enhancer maintenance, and ETV1 binding to ETV1-dependent GIST lineage-specific genes. Thus, FOXF1 is required for GIST cell growth and survival.

The present study confirms that MITF is a novel key driver of KIT oncogenic program in GIST. Apart from our previous work ⁶, the role of MITF in GIST has remained elusive. In this report, we characterize MITF isoforms and the impact of MITF on GIST cell survival in both imatinib-sensitive and imatinib-resistant GIST cells *in vitro* and *in vivo*.

2. MATERIALS AND METHODS

2.1. MITF isoforms in publicly available databases from GIST cell lines and patients.

2.1.1. Expression of MITF isoforms

GIST cell lines (GIST-T1, GIST-T1/670, GIST-T1/816, and GIST882) RNAseq data were obtained through the Gene Expression Omnibus (GEO) accession number GSE156680 ³⁰.

Publicly available bulk RNAseq data from GIST patients were used as a validation cohort from the Sequencing Read Archive (SRA) under the accession number PRJNA521803 ³¹.

2.1.2. Molecular classification of GIST patient tumors

For the classification of GIST patient samples in representative molecular groups, we performed a variant calling of KIT and PDGFRA genes to classify the samples from PRJNA521803 in three different categories (**Sheet “PRJNA521803_samples” from “20220426—MITF_isoforms_results.xlsx”**): KIT, PDGFRA and KIT/PDGFRA WT samples (if neither KIT nor PDGFRA pathogenic mutations were detected).

Raw FASTQ files were aligned against the GRCh38 human genome using STAR ³² with default parameters.

After marking duplicated reads from BAM files, we performed a dual variant calling using FreeBayes ³³ and VarDict ³⁴ to improve the detection of complex indels restricted to *KIT* exons 9 and 11. Parameters were customized *ad hoc* for a tumor-only setup following the suggestions of the developers of both algorithms. Variant calls with less than 20x depth of coverage, and 5 reads with the alternate allele or with a variant allele fraction (VAF) below 5% were discarded for the molecular classification of the samples.

Filtered variants were annotated using VEP to prioritize potentially pathogenic variants depending on the clinical annotation of the variants, the prediction of variant pathogenicity by predictors and meta-predictors, the conservation of the regions affected, and biologically relevant domains of the protein.

KIT variants were restricted to exons 9 (extracellular domain) and 11 (juxtamembrane domain) for primary mutations and exons 13/14 (ATP-binding pocket domain) and 17/18 (activation-loop domain) from the kinase domain for secondary mutations in KIT mutant tumors.

PDGFRA pathogenic variants were restricted to exons 12 (juxtamembrane domain), 14 (ATP-binding pocket domain), and 17/18 (activation-loop domain).

2.1.3. Genes expression and MITF isoforms quantification

Raw FASTQ files from GIST cell lines and GIST patient tumors were aligned to the GRCh38 transcriptome (RefSeq transcripts) using STAR with the default parameters suggested by the authors.

Aligned transcriptomes were used to quantify gene expression of KIT, ETV1, MITF; and MITF isoforms using RSEM³⁵ with the Bayesian version of its model to produce posterior mean estimates (PME) and 95% confidence intervals (CI) for the abundance (transcripts per million, TPM) of each isoform.

RefSeq transcript IDs were mapped to representative isoform names (Sheet “MITF_transcript_variants” from “20220426—MITF_isoforms_results.xlsx”).

2.2. Antibodies and reagents

Antibodies used were as follows: Mouse anti-KIT (clone Ab81), mouse anti-BCL2, and mouse anti-CDK2 were purchased from Santa Cruz Biotechnology, Inc (Santa Cruz, CA, USA). Anti-MITF (clone D5G7V), was obtained from Cell Signaling Technology, Inc (Danvers, MA, USA). Mouse anti- β -actin (clone AC-40) was purchased from Sigma (St. Louis, MO, USA). Anti-mouse and anti-rabbit IgG peroxidase Abs were purchased from DAKO (Carpinteria, CA, USA) and Biorad (Hercules, CA, USA), respectively. Rabbit anti-PDGFRA (clone C20) was purchased from Santa Cruz Biotechnology, Inc. (Santa Cruz, CA, USA). Mouse anti- α -tubulin (clone DM1A) was purchased from Sigma (St. Louis, MO, USA). Anti-ETV1 antibody (ER81) (ab81086) and anti-FOXF1 antibody (EPR7971) (ab168383) were obtained from Abcam technology (Abcam, Cambridge, UK).

2.3. Cell culture

Human GIST cell lines GIST882, GIST48, and GIST 48B were kindly provided by Dr. S. Bauer (University Duisburg-Essen, Medical School, Essen, Germany). Imatinib-sensitive GIST882 cells³⁶ were maintained in RPMI 1640 media (Lonza; Basel, Switzerland) supplemented with 15% fetal bovine serum (FBS) (Attendbio; Barcelona, Spain), 1% L-glutamine (Lonza), 50 units/ml penicillin, and streptomycin (Lonza). Imatinib-resistant GIST 48³⁷ and GIST48 B³⁸ cells were maintained in Ham's F-10 media (Lonza) supplemented with 15% FBS, 1% L-glutamine, 50 units/ml penicillin, and streptomycin, 30 mg/ml bovine pituitary extract and 0.5% MITO+ Serum Extender (Fischer Scientific, Pittsburg, PA). GIST430/654 (Bauer et al., 2007) were cultured in IMDM media supplemented with 15% FBS, 1% L-glutamine, 50 units·mL⁻¹ penicillin and streptomycin, and an additional 200 nM imatinib mesylate (Sigma-Aldrich) to maintain selective pressure. Imatinib-sensitive GIST-T1 and imatinib-resistant GIST-T1-derived sublines GIST-T1/670 and GIST-T1/816 have been published previously³⁹. The human mast cell line, HMC-1 was obtained from J. H. Butterfield (Mayo Clinic, Rochester, MN) and was grown in Iscove's media supplemented with 10% heat-inactivated FBS, penicillin (100 U/ml), and streptomycin (100 µg/ml)⁴⁰. Mycoplasma test is performed routinely in all cell lines used. All cell lines were periodically credentialed by Sanger sequencing of known KIT mutations.

2.4. RT-PCR analysis of MITF isoforms in GIST cell lines

Total RNA was extracted with a QIAGEN RNA Isolation Kit (QIAGEN USA) from all types of GIST cells and HMC-1 cells, which were used as a control. cDNA was generated by reverse transcription using the Transcriptor High Fidelity cDNA Synthesis Kit (ROCHE, CA. USA). RT-PCR was performed using the Fast start High Fidelity PCR System (ROCHE, CA. USA) to identify MITF isoforms A, C, H, CM, and M and was performed following instructions with slight modifications¹⁷. HPRT F: TGACCTGATTTATTTTGCATACC, R: CGAGCAAGACGTTTCAGTCCT, were used as a control. PCR products were separated by electrophoresis in 2% agarose gel TopVision agarose (Thermo Waltham, MA USA). PCR products were detected by the transillumination UV ChemiDoc™ Touch Imaging System (Bio-Rad Laboratories, Inc. USA).

2.5. Lentiviral transduction and generation of transfectants

Lentiviral particles to silence *MITF* gene expression were generated according to the manufacturer's instructions (Sigma, St. Louis, MO, USA). Non-target sequence was as follows: 5' CCGGCAACAAGATGAAGAGCACCAACTCGAGTTGGTGCTCTTCATCTTGTTGTTTT 3'. The MITF-specific shRNA sequences were as follow: shRNA MITF-1 sequence: CCGGCGTGGACTATATCCGAAAGTTCTCGAGAACTTTCCGATATAGTCCACGTTTTT; shRNA MITF-2 sequence: CCGGCGGGAAACTTGATTGATCTTTCTCGAGAAAGATCAATCAAGTTTCCC GTTTTT; shRNA MITF-3 sequence: CCGGGGGAGCTCACAGCGTGTATTTCTCGAGAAATACACGCTGTGAGCTC CTTTTTTG. Lentiviral transduction was performed as described in ⁵ with slight modifications. GIST cells were transduced in the presence of 8 µl/ml of Polybrene (Santa Cruz), and puromycin selection at 1 to 2 µg/ml was carried out 1 day after transduction. Cells were maintained in puromycin until experiments were performed. MITF silencing was checked on different days. MITF silencing was optimal on days 5 and 7, and experiments were carried out.

2.6. Cell viability, proliferation, and caspase activity

Cell viability was measured using Crystal violet and WST-1 assays. Crystal violet dye was used to measure the percentage of surviving attached cells by measuring the percentage of crystal violet OD as explained elsewhere ⁴¹. This assay was performed on the 2nd, 5th, and 7th days after lentiviral transduction.

Cell proliferation was measured using the WST-1 assay. Transduced cell lines were seeded in 96-well plates (0.2×10⁵ cells/well). After 24 h of incubation, they were selected with puromycin (2µg/ml), and cell viability was evaluated with a colorimetric assay (WST-1 based) (Version 17 Cell Proliferation Reagent WST-1, Roche Diagnostics, Germany) on the 2nd, 5th, and 7th day after transduction.

Caspase activity was assayed using the Caspase-Glo™ 3/7 Assay (Promega, San Luis Obispo, CA, USA), according to the manufacturer's instructions. This assay was performed on the 5th and 7th days after lentiviral transduction.

2.7. Western blotting

Transduced cells were lysed on the 5th and 7th days post-lentiviral infection. The total protein concentrations were determined using the Protein Assay Dye Bio-Rad Kit (Bio-Rad Laboratories, Inc. USA) according to the manufacturer's recommendations. Electrophoresis and protein blotting was performed using NuPage™ 4-12%Bis-Tris Gel, 1.5 mm*15 w (Invitrogen, USA), and electrotransferred to polyvinylidene difluoride (PVDF) membranes (Millipore, Bedford, MA, USA). Western blotting with the indicated antibodies was carried out as previously described^{42 6}. In all blots, proteins were visualized by enhanced chemiluminescence (Western Bright™ ECL, Advansta, USA).

2.8. Cell cycle analysis by Flow cytometry

GIST cells were harvested on the 5th and 7th days after lentiviral transduction. The cells were fixed with 70% ethanol at 4°C overnight. Cells were washed twice with cold PBS buffer, and resuspended in propidium iodide staining solution buffer for 30 min, as described elsewhere⁴³. Data were acquired in a FACS Calibur and analyzed using model Dean/Jet/Fox FlowJo 7.6 software.

2.9. *In vivo* xenografts

MITF knock-down *in vivo*. Heterotopic GIST-T1 xenografts were generated in NMRInu/nu mice and maintained as previously described³⁰. The treatments were not blind to the investigator, and no randomization was used. Tumor volume was assessed three times per week once tumors were measured. Bodyweight was assessed once per week. Mice were euthanized when tumor volume in any treatment arm reached 1200 mm³. Tumors were resected and photographed. All animal studies were conducted according to ARRIVE guidelines and the three Rs rules of replacement, reduction, and refinement. All *in vivo* work was conducted following approved protocols from the Institutional Animal Care and Use Committee.

2.10. Statistical data analysis

All *in vitro* experiments have been performed several times ($n > 5$). *In vivo* experiments: GIST-T1 cells transduced with empty ($n = 4$) and shRNA targeting MITF ($n = 14$) vectors were xenografted *in vivo*. All results are expressed as mean \pm standard error of the mean (SEM). After determining the normal distribution of the samples and variance analysis, an unpaired student's t-test was used to determine significant differences (p-value) between the two experimental groups. A one-way ANOVA test was used to determine significant differences (p-value) between several experimental groups.

3. RESULTS

3.1. MITF isoforms in GIST

In previous work, we showed that MITF was expressed in GIST cell lines and primary tumor patients' samples⁶. However, there are several MITF isoforms described, differing in their exon 1 and sharing common downstream exons from 2 to 9¹³. Thus, we first analyzed MITF isoforms in GIST patient tumor samples using publicly available bulk RNAseq³¹. GISTs were classified accordingly to KIT and PDGFRA molecular status. MITF A was the most predominant isoform, and it was found expressed both KIT and PDGFRA GIST patients (Figures 1 A and C). Expression levels of total MITF were also analyzed in relation to KIT and ETV1 in the same patient samples. Interestingly, total MITF expression levels were co-expressed with KIT and ETV-1 in most cases (Figures 1 B and D). A positive correlation coefficient between these proteins in these patients was found (Table I). Additionally, MITF isoforms were also validated in GIST cell lines. To identify MITF isoforms in imatinib-sensitive and -resistant GIST cell lines, cDNA was obtained from cultured cells growing in their specific culture media. Our experimental setup is based on a previous study on mast cells¹⁷. We characterized MITF A, H, C, CM, and M by RT-PCR (Supplementary Figure 1). MITF isoforms A and H were expressed in all GIST cells. Interestingly we found MITF C expression in GIST 430/654 only. MITF M and MITF CM were not found expressed in the GIST cell lines used. Accordingly, analysis of MITF isoforms in bulk RNA sequencing data from GIST cell lines also demonstrated the predominance of MITF A expression over other isoforms³⁰ (Supplementary figure 2). Together, this analysis supports previous findings in the literature where MITF A is highly expressed in non-melanoma cancer cells⁴⁴.

3.2. MITF silencing reduces KIT, BCL2, and CDK2 expression in GIST cell lines

To analyze the role of MITF in GISTs, MITF gene expression was stably silenced by lentivirus shRNAs in the imatinib-sensitive GIST cell line, GIST T1, and in the imatinib-resistant GIST cell line, GIST 48. Among the three different sequences tested - shRNA MITF-1, shRNA MITF-2, and shRNA MITF-3 - only sequence 3 was effective at day five (Figure 2 A) in both cell lines, although sequences 1 and

3 were effective on day seven (Figure 2B) in both cell lines. Expression levels of KIT were analyzed along with other MITF-dependent targets related to cell survival and cell cycle regulation described in mast cells or melanocytes, such as BCL2 and CDK2. MITF was found to transactivate the *c-kit* gene via binding to the CACCTG motif in the *c-kit* promoter in mast cells⁴⁵. BCL2 was previously reported as a MITF-dependent target regulating cell viability and survival in melanocytes⁴⁶. Furthermore, MITF was stated to upregulate CDK2 expression in melanoma, and depletion of CDK2 suppresses growth and cell cycle progression in melanoma⁴⁷. Interestingly, our results demonstrate that MITF silencing was accompanied by a reduction in KIT, BCL2, and CDK2 expression, thus confirming that they are also MITF-dependent targets in GIST (Figure 2B).

3.3. MITF silencing impairs GIST cell proliferation and the cell cycle.

Next, we explored the role of MITF in GIST proliferation and the cell cycle. Our results showed that MITF silencing was accompanied by a decrease in cell proliferation in GIST-T1 (Figure 3A) and GIST 48 (Figure 3B). The most significant reduction was seen seven days after lentiviral transduction, where MITF expression was undetectable (Figure 2B). As shown above, MITF silenced cells significantly reduced CDK2 expression. To further demonstrate the functional consequence of MITF silencing in the CDK2 context, the cell cycle was analyzed by flow cytometry. Our results revealed a significant accumulated cell population indicative of cell cycle arrest in the G2/M phase in MITF-silenced GIST-T1 (Figure 4 A) and S phase in MITF-silenced GIST 48 (Figure 4 B) on the 7th-day post-transduction.

3.4. MITF silencing induces caspase 3/7 activation in GIST cell lines.

To elucidate whether a reduction in proliferation and cell cycle impairment was leading to impairment in cell viability and apoptosis induction, we performed a viability assay and measured Caspase 3/7 activation in MITF silenced cells on the 5th and 7th-day post-transduction, where MITF silencing was revealed to be more significant. Our results demonstrated a decrease in cell viability that correlated with an increase in caspase 3/7 activity in both cell lines (Figure 5). This impact of MITF knock-down parallels the reduction in KIT and BCL-2 expression, as we observed before (Figure 2B).

3.5. MITF silencing downregulates ETV1 expression in GIST cell lines.

A mechanism connecting MITF and ETV1 in melanocytes has been suggested. DNA amplifications involving the *ETV1* locus occur frequently in melanoma. Interestingly, ETV1 has been found to indirectly increase MITF expression and this fact seems to be necessary for ETV1 oncogenicity in melanoma⁴⁸. Since ETV1 is a master regulator of ICC-GIST-specific transcription programs and is required for GIST growth²⁷, we next analyzed ETV1 expression after MITF silencing. Interestingly, a decrease in ETV1 expression was observed on the 7th-day post-transduction in imatinib-sensitive and resistant cell lines (Figure 6). It is known that ETV1 expression is regulated by KIT and, together with KIT, forms a positive feedback circuit to regulate the expression of target genes in GIST²⁸. Since KIT is reduced after MITF silencing, this may be the cause underlying the decrease in ETV1 expression. To obtain further insight into this pathway, we additionally studied MITF silencing in GIST48B cells, a subline of GIST 48, which, despite retaining the activating *KIT* mutation, expresses the KIT transcript and protein at essentially undetectable levels^{6,38}. In this context of absent KIT expression, ETV1 was still expressed suggesting that alternative mechanisms of regulation must be activated besides the well-known stabilization of ETV1 mediated through KIT-MAPK signaling²⁸. Recent studies have demonstrated that the FOXF1 also controls the transcriptional activation of ETV1²⁹. In this sense, GIST48B maintains appreciable levels of FOXF1 and therefore may explain the ETV1 expression. Interestingly, MITF silencing in GIST48B also leads to a clear ETV1 reduction on the day 7 (Figure 7B). Accordingly, MITF shRNA silencing results in decreased GIST48B cell proliferation (Figure 7C) and cell cycle arrest (Figure 7D), together with a concomitant decrease in BCL2 and CDK2 expression (Figure 7A).

Importantly, our results demonstrate that MITF silencing downregulates KIT and ETV1 expression independent of FOXF1 in both imatinib-sensitive and resistant GIST cells (Figure 6, Figure 7). Therefore, MITF activity in GIST appears to be mediated, at least partially, by the co-regulation of the ETV1 transcription factor.

3.6. MITF silencing prevents tumor growth *in vivo*

To further demonstrate the role of MITF silencing in GIST, we assessed tumor growth *in vivo* using GIST-T1 transduced with NT shRNA or MITF shRNA-3. MITF protein levels were evaluated on days 5 and 7 after puromycin selection in cell lines in parallel to the xenograft experiments, further confirming that transfected cells had efficiently lost MITF expression (Figures 8A and 8B). Consistent with the results obtained *in vitro*, a significant delay in tumor growth in GIST-T1 xenograft of MITF shRNA transduced GIST cells was observed *in vivo* (Figures 8C and 8D). Altogether, our data demonstrate that MITF expression is required for tumor growth in GIST.

4. DISCUSSION

Activating KIT mutations in GIST turns KIT into the critical therapeutic target for the treatment of GIST. Therefore, imatinib, a tyrosine kinase inhibitor (TKI) targeting KIT activation, is the first-line treatment for GIST ⁴. However, little is known about KIT regulation and KIT signaling intermediates in GIST. Here we report that microphthalmia-associated transcription factor (MITF) functions as an oncogenic transcription factor in GIST by promoting cell survival and tumor growth. MITF belongs to the MITF/TFE family of basic helix-loop-helix leucine zipper (b-HLH-LZ) transcription factors which include TFEB, TFE3, and TFEC. The b-HLH-LZ recognizes the E-box (CANNTG) motifs in the promoter region of target genes involved in a range of biological processes, including cell survival, proliferation, invasion, and senescence. The role of MITF has been widely studied in melanoma ¹⁵ but it remains unknown in GIST. To delve into the role of MITF in GIST, we first analyzed MITF isoforms expressed in various imatinib-sensitive and resistant GIST cell lines with clinically-representative KIT primary and secondary mutations. Several isoforms have been described with tissue-specific first exons and common exons 2-9, the expression of which reflects a predominantly tissue-specific regulation. In addition, several alternative splicing forms have been described ¹⁶. The characterization of these isoforms is limited, and the total number of alternative MITF transcripts and proteins is currently unknown, so we set up our first approach toward isoform characterization in GIST using a published methodology ¹⁷ and database sources. MITF-A isoform is the most well-represented isoform in GIST patients independently of the driver mutation. MITF A and MITF H were found expressed in all the imatinib-sensitive and imatinib-resistant GIST cell lines assessed. MITF A is the longest isoform and is ubiquitously expressed ⁴⁹. MITF H is expressed in heart ⁵⁰, regulating the expression of myosin light-chain 1a (MLC-1a) in cardiomyocytes. The specific function of each isoform needs to be addressed. The isoform-specific knock-outs available are restricted to M and A isoforms, showing that the M isoform is critical for the generation of melanocytes in the epidermis and pigmentation. In contrast, the A isoform plays a limited role in this phenotype ¹⁸. Knocking out MITF A also produces a reduced number of nephrons, MITF A overexpressing mice, and,

unexpectedly, MITF M knock-out mice show both enlarged kidneys^{18,51}. Thus, GIST expresses specific MITF isoforms.

We previously reported that MITF overexpression in GIST significantly reverses the apoptotic phenotype produced by SH3BP2 silencing, suggesting the involvement of this transcription factor in pro-survival signals in GIST⁶. In this study, we show that MITF silencing has a pro-apoptotic effect on imatinib-sensitive GIST-T1 and imatinib-resistant GIST48 cell lines. This result correlated with the increased caspase 3/7 levels, confirming a pro-survival role for this factor in GIST. We found that BCL2, an anti-apoptotic BCL2 family member⁵² is positively regulated by MITF in imatinib-sensitive and resistant GIST. These results agree with previous findings showing that cellular apoptosis triggered by MITF disruption can be rescued by BCL2 overexpression in melanocytes and melanoma⁴⁶. Several anti-apoptotic proteins have been reported to be MITF-dependent targets. BIRC7, also called ML-IAP (Melanoma inhibitor of apoptosis), which can inhibit extrinsic and intrinsic apoptotic pathways by interaction with caspases, is upregulated by MITF¹⁴. The anti-apoptotic BCL2A1 has also been identified as a direct target of MITF, suggesting that the MITF-BCL2A1 relationship may be an intrinsic mechanism protecting melanoma cells from drug-induced death⁵³. Selective inhibition of these targets may have therapeutic potential in cancer treatment⁵⁴.

MITF silencing, apart from the pro-apoptotic phenotype in GIST-T1 and GIST-48, results in cell cycle arrest in G2/M and S cell cycle phases, respectively. Concomitantly, CDK2 levels are diminished in silenced cells. Interestingly, CDK2 is a MITF target, and the expression of both is tightly correlated in primary melanoma specimens and predicts susceptibility to CDK2 inhibitors⁴⁷. CDK2 has been described to regulate both G1/S and G2/M transitions⁵⁵. Higher expression of double negative CDK2 caused cell arrest in the mid-S phase, while lower expression progressed well through an early and mid-S phase but still arrested in late S/G2⁵⁵, suggesting that the levels of active CDK2 can be key in the different phases. More recently, CDK2 absence has been shown to slow S/G2 progression in colorectal carcinoma⁵⁶. The fact that we see differences in the cell cycle after MITF silencing in GIST T1 versus GIST 48 and GIST48B may also be due to differences in the cell growth rates of these cell lines. GIST-T1 grows much

faster (almost three times) than GIST 48 or GIST48B. Thus GIST-T1 enters the S phase faster and progresses well through an early and mid-S phase but arrests in late S/G2. The analysis of the role and regulation of CDK2 in GIST deserves further consideration.

Part of the apoptotic phenotype described in MITF silencing can be due to a decrease in ETV1 expression. ETV1 is required for pro-survival signals and is an essential transcription factor in oncogenic KIT signaling pathways in GIST²⁷. The KIT cascade, including MAPK activation downstream, lengthens ETV1 stability and collaborates with ETV1 to support tumorigenesis²⁸. The fact that MITF silencing also leads to a reduction in KIT expression may indirectly explain the decrease in ETV1. Interestingly, MITF silencing in GIST 48B, where KIT signaling is absent, leads to an apparent ETV1 reduction. Our results link MITF and ETV1 expression in GIST. Indeed ETV1 overexpression increases MITF expression, and this event is necessary for ETV1-dependent oncogenicity in melanoma⁴⁸. Our data show that GIST48B expresses FOXF1, which may explain ETV1 expression in the absence of KIT expression and signaling. Lately, it was discovered that FOXF1 is a pioneer factor that transcriptionally regulates ETV1, KIT, and the ICC/GIST lineage-specific genes and is located upstream of them²⁸. Thus, FOXF1 knock-down downregulates KIT and ETV1 expression, however, KIT and ETV1 expression and signaling do not affect FOXF1 expression²⁸. Our data show that MITF silencing results in a reduction of KIT and ETV1 expression, and FOXF1 expression remains unaltered in GIST-T1 and slightly reduced in GIST 48 and GIST 48B, suggesting that FOXF1 should be at the top of the hierarchy or in a different pathway. The analysis of the transcriptome in FOXF1-silenced GIST48 cells shows a slight reduction in MITF expression (GSE 106625, Ran *et al.*, 2018), suggesting that both factors may act in different pathways. Altogether, our data indicate that MITF regulates KIT and ETV-1. Further studies are required to fathom the common regulation of these transcription factors.

Our study shows, for the first time, that KIT expression is regulated by MITF in GIST, concurring with previous data showing that MITF regulates KIT expression by binding to its promoter in mast cells⁴⁵. Moreover, KIT signaling regulates MITF mRNA stability via two microRNAs, miR381 and miR539, which bind to the 3'UTR (untranslated region) of MITF mRNA, preventing its translation to protein in mast

cells ⁵⁷. This reciprocal regulation is also found in GIST, where inhibition of KIT signaling with imatinib reduces MITF expression ⁶. To reveal whether this regulation is direct, indirect, or both deserve further consideration.

Altogether, our data demonstrate that MITF is required for cell proliferation and survival *in vitro* and tumor growth *in vivo*. Targeting MITF may help break the positive feedback loop between KIT and ETV1 and indirectly target KIT expression independently of the mutations found in the tyrosine kinase receptor.

DATA AVAILABILITY

The datasets used and analyzed during the current study are available in the article and supplementary files or from the corresponding author at reasonable request.

REFERENCES

- 1 Demetri GD, von Mehren M, Antonescu CR, DeMatteo RP, Ganjoo KN, Maki RG *et al.* NCCN Task Force Report: Update on the Management of Patients with Gastrointestinal Stromal Tumors. *J Natl Compr Cancer Netw* 2010; **8**: S-1-S-41.
- 2 Beham AW, Schaefer I-M, Schüler P, Cameron S, Michael Ghadimi B. Gastrointestinal stromal tumors. *Int J Colorectal Dis* 2012; **27**: 689–700.
- 3 Serrano C, George S. Gastrointestinal Stromal Tumor: Challenges and Opportunities for a New Decade. *Clin Cancer Res* 2020; **26**: 5078–5085.
- 4 Demetri GD, von Mehren M, Blanke CD, Van den Abbeele AD, Eisenberg B, Roberts PJ *et al.* Efficacy and Safety of Imatinib Mesylate in Advanced Gastrointestinal Stromal Tumors. *N Engl J Med* 2002; **347**: 472–480.
- 5 Ainsua-Enrich E, Serrano-Candelas E, Álvarez-Errico D, Picado C, Sayós J, Rivera J *et al.* The Adaptor 3BP2 Is Required for KIT Receptor Expression and Human Mast Cell Survival. *J Immunol* 2015; **194**: 4309–4318.
- 6 Serrano-Candelas E, Ainsua-Enrich E, Navinés-Ferrer A, Rodrigues P, García-Valverde A, Bazzocco S *et al.* Silencing of adaptor protein SH 3 BP2 reduces KIT / PDGFRA receptors expression and impairs gastrointestinal stromal tumors growth. *Mol Oncol* 2018; **12**: 1383–1397.
- 7 Oppezzo A, Rosselli F. The underestimated role of the microphthalmia-associated transcription factor (MITF) in normal and pathological haematopoiesis. *Cell Biosci* 2021; **11**: 1–15.
- 8 Kawakami A, Fisher DE. The master role of microphthalmia-associated transcription factor in melanocyte and melanoma biology. *Lab Investig* 2017; **97**: 649–656.
- 9 Kim JH, Jin HM, Kim K, Song I, Youn BU, Matsuo K *et al.* The Mechanism of Osteoclast Differentiation Induced by IL-1. *J Immunol* 2009; **183**: 1862–1870.
- 10 Zhao H, Zhang J, Shao H, Liu J, Jin M, Chen J *et al.* MiRNA-340 inhibits osteoclast differentiation via repression of MITF. *Biosci Rep* 2017; **37**: 1–8.
- 11 Wen B, Li S, Li H, Chen Y, Ma X, Wang J *et al.* Microphthalmia-associated

- transcription factor regulates the visual cycle genes *Rlbp1* and *Rdh5* in the retinal pigment epithelium. *Sci Rep* 2016; **6**: 1–9.
- 12 Levy C, Khaled M, Fisher DE. MITF: master regulator of melanocyte development and melanoma oncogene. *Trends Mol Med* 2006; **12**: 406–414.
 - 13 Hartman ML, Czyz M. MITF in melanoma: Mechanisms behind its expression and activity. *Cell Mol Life Sci* 2015; **72**: 1249–1260.
 - 14 Hartman ML, Czyz M. Pro-Survival Role of MITF in Melanoma. *J Invest Dermatol* 2015; **135**: 352–358.
 - 15 Goding CR, Arnheiter H. MITF—the first 25 years. *Genes Dev* 2019; **33**: 983–1007.
 - 16 Vu HN, Dilshat R, Fock V, Steingrímsson E. User guide to MIT-TFE isoforms and post-translational modifications. *Pigment Cell Melanoma Res* 2021; **34**: 13–27.
 - 17 Shiohara M, Shigemura T, Suzuki T, Tanaka M, Morii E, Ohtsu H *et al.* MITF-CM, a newly identified isoform of microphthalmia-associated transcription factor, is expressed in cultured mast cells. *Int J Lab Hematol* 2009; **31**: 215–226.
 - 18 Flesher JL, Paterson-Coleman EK, Vasudeva P, Ruiz-Vega R, Marshall M, Pearlman E *et al.* Delineating the role of MITF isoforms in pigmentation and tissue homeostasis. *Pigment Cell Melanoma Res* 2020; **33**: 279–292.
 - 19 Garraway LA, Widlund HR, Rubin MA, Getz G, Berger AJ, Ramaswamy S *et al.* Integrative genomic analyses identify MITF as a lineage survival oncogene amplified in malignant melanoma. *Nature* 2005; **436**: 117–122.
 - 20 Bertolotto C, Lesueur F, Giuliano S, Strub T, De Lichy M, Bille K *et al.* A SUMOylation-defective MITF germline mutation predisposes to melanoma and renal carcinoma. *Nature* 2011; **480**: 94–98.
 - 21 Yokoyama S, Woods SL, Boyle GM, Aoude LG, MacGregor S, Zismann V *et al.* A novel recurrent mutation in MITF predisposes to familial and sporadic melanoma. *Nature* 2011; **480**: 99.
 - 22 Cheli Y, Giuliano S, Botton T, Rocchi S, Hofman V, Hofman P *et al.* Mitf is the key molecular switch between mouse or human melanoma initiating cells and their differentiated progeny. *Oncogene* 2011; **30**: 2307–2318.
 - 23 Cheli Y, Giuliano S, Fenouille N, Allegra M, Hofman V, Hofman P *et al.* Hypoxia and MITF control metastatic behaviour in mouse and human melanoma cells. *Oncogene* 2012; **31**: 2461–2470.
 - 24 Müller J, Krijgsman O, Tsoi J, Robert L, Hugo W, Song C *et al.* Low MITF/AXL ratio predicts early resistance to multiple targeted drugs in melanoma. *Nat Commun* 2014; **5**: 5712.
 - 25 Carreira S, Goodall J, Denat L, Rodriguez M, Nuciforo P, Hoek KS *et al.*

- Mitf regulation of Dia1 controls melanoma proliferation and invasiveness. *Genes Dev* 2006; **20**: 3426–3439.
- 26 Rambow F, Marine JC, Goding CR. Melanoma plasticity and phenotypic diversity: therapeutic barriers and opportunities. *Genes Dev* 2019; **33**: 1295.
- 27 Chi P, Chen Y, Zhang L, Guo X, Wongvipat J, Shamu T *et al.* ETV1 is a lineage survival factor that cooperates with KIT in gastrointestinal stromal tumours. *Nature* 2010. doi:10.1038/nature09409.
- 28 Ran L, Sirota I, Cao Z, Murphy D, Chen Y, Shukla S *et al.* Combined Inhibition of MAP Kinase and KIT Signaling Synergistically Destabilizes ETV1 and Suppresses GIST Tumor Growth. *Cancer Discov* 2015; **5**: 304–315.
- 29 Ran L, Chen Y, Sher J, Wong EWP, Murphy D, Zhang JQ *et al.* FOXF1 Defines the Core-Regulatory Circuitry in Gastrointestinal Stromal Tumor. *Cancer Discov* 2018; **8**: 234–251.
- 30 García-Valverde A, Rosell J, Sayols S, Gómez-Peregrina D, Pilco-Janeta DF, Olivares-Rivas I *et al.* E3 ubiquitin ligase Atrogin-1 mediates adaptive resistance to KIT-targeted inhibition in gastrointestinal stromal tumor. *Oncogene* 2021; : 1–13.
- 31 Vitiello GA, Bowler TG, Liu M, Medina BD, Zhang JQ, Param NJ *et al.* Differential immune profiles distinguish the mutational subtypes of gastrointestinal stromal tumor. *J Clin Invest* 2019; **129**: 1863–1877.
- 32 Dobin A, Davis CA, Schlesinger F, Drenkow J, Zaleski C, Jha S *et al.* STAR: ultrafast universal RNA-seq aligner. *Bioinformatics* 2013; **29**: 15.
- 33 Garrison E, Marth G. Haplotype-based variant detection from short-read sequencing. 2012. doi:10.48550/arxiv.1207.3907.
- 34 Lai Z, Markovets A, Ahdesmaki M, Chapman B, Hofmann O, McEwen R *et al.* VarDict: a novel and versatile variant caller for next-generation sequencing in cancer research. *Nucleic Acids Res* 2016; **44**: e108.
- 35 Li B, Dewey CN. RSEM: Accurate transcript quantification from RNA-Seq data with or without a reference genome. *BMC Bioinformatics* 2011; **12**: 1–16.
- 36 Tuveson DA, Willis NA, Jacks T, Griffin JD, Singer S, Fletcher CDM *et al.* STI571 inactivation of the gastrointestinal stromal tumor c-KIT oncoprotein: Biological and clinical implications. *Oncogene* 2001; **20**: 5054–5058.
- 37 Bauer S, Duensing A, Demetri GD, Fletcher JA. KIT oncogenic signaling mechanisms in imatinib-resistant gastrointestinal stromal tumor: PI3-kinase/AKT is a crucial survival pathway. *Oncogene* 2007; **26**: 7560–7568.
- 38 Mühlenberg T, Zhang Y, Wagner AJ, Grabellus F, Bradner J, Taeger G *et al.* Inhibitors of Deacetylases Suppress Oncogenic KIT Signaling, Acetylate HSP90, and Induce Apoptosis in Gastrointestinal Stromal Tumors. *Cancer*

- Res* 2009; **69**: 6941–6950.
- 39 Serrano C, Mariño-Enríquez A, Tao DL, Ketzer J, Eilers G, Zhu M *et al.* Complementary activity of tyrosine kinase inhibitors against secondary kit mutations in imatinib-resistant gastrointestinal stromal tumours. *Br J Cancer* 2019; **120**: 612–620.
 - 40 Nilsson G, Blom T, Kusche-Gullberg M, Kjellen L, Butterfield JH, Sundström C *et al.* Phenotypic Characterization of the Human Mast-Cell Line HMC-1. *Scand J Immunol* 1994; **39**: 489–498.
 - 41 Feoktistova M, Geserick P, Leverkus M. Crystal Violet Assay for Determining Viability of Cultured Cells. *Cold Spring Harb Protoc* 2016; **2016**: pdb.prot087379.
 - 42 Álvarez-Errico D, Oliver-Vila I, Ainsua-Enrich E, Gilfillan AM, Picado C, Sayós J *et al.* CD84 Negatively Regulates IgE High-Affinity Receptor Signaling in Human Mast Cells. *J Immunol* 2011; **187**: 5577–5586.
 - 43 Pozarowski P, Darzynkiewicz Z. Analysis of Cell Cycle by Flow Cytometry. In: *Checkpoint Controls and Cancer*. Humana Press: New Jersey, 2004, pp 301–312.
 - 44 Samatiwat P, Takeda K, Satarug S, Ohba K, Kukongviriyapan V, Shibahara S. Induction of MITF expression in human cholangiocarcinoma cells and hepatocellular carcinoma cells by cyclopamine, an inhibitor of the Hedgehog signaling. *Biochem Biophys Res Commun* 2016; **470**: 144–149.
 - 45 Tsujimura T, Morii E, Nozaki M, Hashimoto K, Moriyama Y, Takebayashi K *et al.* Involvement of Transcription Factor Encoded by the mi Locus in the Expression of c-kit Receptor Tyrosine Kinase in Cultured Mast Cells of Mice. *Blood* 1996; **88**: 1225–1233.
 - 46 McGill GG, Horstmann M, Widlund HR, Du J, Motyckova G, Nishimura EK *et al.* Bcl2 regulation by the melanocyte master regulator Mitf modulates lineage survival and melanoma cell viability. *Cell* 2002; **109**: 707–718.
 - 47 Du J, Widlund HR, Horstmann MA, Ramaswamy S, Ross K, Huber WE *et al.* Critical role of CDK2 for melanoma growth linked to its melanocyte-specific transcriptional regulation by MITF. *Cancer Cell* 2004; **6**: 565–576.
 - 48 Jané-Valbuena J, Widlund HR, Perner S, Johnson LA, Dibner AC, Lin WM *et al.* An Oncogenic Role for ETV1 in Melanoma. *Cancer Res* 2010; **70**: 2075–2084.
 - 49 Steingrímsson E, Moore KJ, Lamoreux ML, Ferré-D’Amaré AR, Burley SK, Sanders Zimring DC *et al.* Molecular basis of mouse microphthalmia (mi) mutations helps explain their developmental and phenotypic consequences. *Nat Genet* 1994; **8**: 256–263.
 - 50 Tshori S, Sonnenblick A, Yannay-Cohen N, Kay G, Nechushtan H, Razin E. Microphthalmia Transcription Factor Isoforms in Mast Cells and the Heart. *Mol Cell Biol* 2007; **27**: 3911.

- 51 Phelep A, Laouari D, Bharti K, Burtin M, Tammaccaro S, Garbay S *et al.* MITF – A controls branching morphogenesis and nephron endowment. *PLoS Genet* 2017; **13**: 1–25.
- 52 Kalkavan H, Green DR. MOMP, cell suicide as a BCL-2 family business. *Cell Death Differ* 2018; **25**: 46–55.
- 53 Haq R, Yokoyama S, Hawryluk EB, Jönsson GB, Frederick DT, McHenry K *et al.* BCL2A1 is a lineage-specific anti-apoptotic melanoma oncogene that confers resistance to BRAF inhibition. *Proc Natl Acad Sci U S A* 2013; **110**: 4321–4326.
- 54 Li X, Dou J, You Q, Jiang Z. Inhibitors of BCL2A1/Bfl-1 protein: Potential stock in cancer therapy. *Eur J Med Chem* 2021; **220**: 113539.
- 55 Hu B, Mitra J, van den Heuvel S, Enders GH. S and G 2 Phase Roles for Cdk2 Revealed by Inducible Expression of a Dominant-Negative Mutant in Human Cells . *Mol Cell Biol* 2001; **21**: 2755–2766.
- 56 Bačević K, Lossaint G, Achour TN, Georget V, Fisher D, Dulić V. Cdk2 strengthens the intra-S checkpoint and counteracts cell cycle exit induced by DNA damage. *Sci Rep* 2017; **7**. doi:10.1038/s41598-017-12868-5.
- 57 Lee Y-N, Brandal S, Noel P, Wentzel E, Mendell JT, McDevitt MA *et al.* KIT signaling regulates MITF expression through miRNAs in normal and malignant mast cell proliferation. *Blood* 2011; **117**: 3629–3640.

ACKNOWLEDGEMENTS

We are indebted to the Cytomics core facility of the Institut d'Investigacions Biomèdiques August Pi i Sunyer (IDIBAPS) for their technical support.

AUTHOR CONTRIBUTIONS

E.P-P, E.S-C, and M.M. conceived the experiments and wrote the manuscript, E.P-P and A.G.V performed the experiments, A.N.F, M.G, J.R., and D.G-P. provided technical support, C.S. provided reagents and technical support, and M.M. secured funding. All authors reviewed the manuscript.

FUNDING

This study has been funded by grants from the Spanish Ministry of Science, Innovation and Universities and European Regional Development Fund/European Social Fund "Investing in your future": RTI2018-096915-B100 (M.M.) and PID2021-122898OB-100 (M.M.); PERIS SLT006/17/221 (C.S.), ISCIII PI19_01271 (C.S.) and ISCIII FI20/00275 (D. G-P).

COMPETING INTEREST

CS has received research funding (institution) from Karyopharm, Pfizer, Inc, Deciphera Pharmaceuticals, and Bayer AG; consulting fees (advisory role) from CogentBio, Immunicum AB, Deciphera Pharmaceuticals, and Blueprint Medicines; payment for lectures from PharmaMar, Bayer AG and Blueprint Medicines; and travel grants from PharmaMar, Pfizer, Bayer AG, Novartis, and Lilly.

The remaining authors have declared that no conflict of interest exists.

FIGURE LEGENDS

Figure 1. Expression of MITF isoforms in GIST patients. (A) MITF isoform percentage distributions for GIST tumor samples separated by molecular groups (KIT, PDGFRA, KIT/PDGFRA wild-type (WT)). (B) KIT, ETV1, and MITF gene expression distributions in GIST tumor samples separated by molecular groups (KIT, PDGFRA, KIT/PDGFRA WT). (C) Hierarchically-clustered heatmap showing MITF isoform expression profiles of all GIST tumor samples from the same patients' cohort. (D) Hierarchically-clustering heatmap showing KIT, ETV1, and MITF gene expression profiles of GIST tumor samples from patients' cohort. The data was obtained from the Sequencing Real Archive (SRA) under the accession number PRJNA521803 ³¹.

Figure 2. MITF silencing reduces KIT, BCL2, and CDK2 expression. (A) MITF expression protein in GIST-T1 and GIST48 lysates were evaluated by Western blotting protein in cells transduced with control NT (non-target) shRNA, MITF shRNA-1, MITF shRNA-2, and MITF sh RNA-3 at 5 days. (B) Lysates from GIST-T1 and GIST48 cells transduced by the sequences MITF shRNA-1, MITF shRNA-3, and NT shRNA were analyzed by Western blot to determine levels of KIT, MITF, BCL2, and CDK2 at 7 days; β -actin was used as a loading control. Blots are representative of several experiments (n>3).

Figure 3. MITF silencing impairs cell proliferation. Cell proliferation assay was performed by WST-1, and sequences NT shRNA, MITF shRNA-1, and MITF shRNA-3 were measured on the 2nd, 5th, and 7th day after lentiviral transduction (A) GIST T-1 and (B) GIST 48. Statistical significance (* p <0.05, ** p <0.01, *** p <0.001); One-way ANOVA with Bonferroni's post hoc test; n = 3 each experimental group; mean \pm SEM) is relative to NT shRNA at each time point.

Figure 4. MITF silencing impairs the cell cycle. Cell cycle assay was performed by propidium iodide by FACS in infected cells 7 days after lentiviral transduction with NT(non-target) shRNA, MITF shRNA-1, and MITF shRNA-3 sequences. Results were analyzed by Dean/Jett/Fox model Flow jo 7.0 software (A) GIST T-1 and (B) GIST 48. Statistical significance (*p<0.05, *** p <0.001, ****p<0.0001); Unpaired T-test; n = 3 each experimental group mean \pm SEM) is relative to NT shRNA at each time point.

Figure 5. MITF induces apoptosis by caspases in GIST cells. (A) GIST-T1 and (B) GIST 48; cell lines were transduced either with NT shRNA or MITF shRNA-3, sample lysates were analyzed for MITF expression protein 5 and 7 days after lentiviral transduction, β -actin was used as a loading control. A viability assay was performed on (C) GIST-T1 and (D) GIST 48 with cristal violet on the 2nd, 5th, and 7th days after lentiviral transduction. Statistical significance (**** $p < 0.0001$; One-way ANOVA with Bonferroni's *post hoc* test, mean \pm SEM; $n = 3$) is relative to NT shRNA at each time point. Caspase 3/7 activity was measured on the 5th and 7th-day post-lentiviral transduction (E) GIST-T1 and (F) GIST 48. Statistical significance (* $p < 0.05$, ** $p < 0.01$, *** $p < 0.001$; unpaired T-test; $n = 3$ each experimental group mean \pm SEM) is relative to NT shRNA at each time point.

Figure 6. MITF silencing induces ETV1 downregulation in GISTs. Western blots were performed to analyze protein levels for KIT, MITF, ETV1, and FOXF1 on the 7th day post-lentiviral transduction in (A) GIST-T1 and (B) GIST 48; α -tubulin and β -actin were used as loading controls.

Figure 7. MITF silencing affects viability and the cell cycle in GIST 48 B cells. (A) MITF sh RNA-3 was used for silencing GIST 48B. Lysates were analyzed by Western blot to determine levels of PDGFRA, MITF, CDK2, and BCL2; β -actin was used as a loading control on the 7th-day post-transduction. (B) Lysates were analyzed by Western blot to determine FOXF1 and ETV1 levels, and tubulin was used as a loading control on the 7th-day post-transduction. (C) Cell proliferation was verified by WST-1 on the 2nd, 5th, and 7th days after transduction. Statistical significance (**** $p < 0.0001$; One-way ANOVA with Bonferroni's *post hoc* test, mean \pm SEM; $n = 3$) is relative to NT shRNA at each time point. (D) Cell cycle assay was performed by FACS in GIST transfected NT shRNA and MITF shRNA-3 sequences on the 7th day. Results were analyzed using Dean/Jett/Fox model Flow jo 7.0 software. Statistical significance (* $p < 0.05$, unpaired T-test; mean \pm SEM; $n = 3$) is relative to NT shRNA at each time point.

Figure 8. MITF silencing causes a reduction in GIST tumor growth. (A) GIST-T1 was transduced with either control NT (non-target) shRNA or MITF shRNA-3, and the efficiency of MITF silencing was assessed by western blot. On the 5th and 7th days after lentiviral transduction, α - tubulin was used as a loading control.

(B) To verify the percentage of viable cells *in vitro*, a WST-1 assay was performed in transduced cells and was measured on the 2nd, 5th, and 7th days after shRNA lentiviral transduction. (C) GIST-T1 cells transduced with empty (n=4) and shRNA targeting MITF (n=14) vectors were xenografted *in vivo*. Tumor volume was assessed three times per week. (D) Representative photograph of the tumors on the 23rd-day post-injection. Statistical significance was assessed using a two-tailed unpaired T-test corrected by multiple comparisons using the Holm-Sidak method. ** < 0.005, *** < 0.001.

TABLE LEGEND:

TABLE I. MITF, ETV1 and KIT correlation in GIST patients. Pearson and Spearman's correlations in GIST patients are shown in Figure 1.

Gene A	Gene B	Pearson correlation		Spearman correlation	
		R	p value	r	p value
KIT	KIT	1,00	0,00E+00	1,00	0,00E+00
KIT	ETV1	0,73	8,91E-14	0,67	0,00E+00
KIT	MITF	0,50	4,61E-06	0,55	0,00E+00
ETV1	KIT	0,73	8,91E-14	0,67	0,00E+00
ETV1	ETV1	1,00	0,00E+00	1,00	0,00E+00
ETV1	MITF	0,57	1,08E-07	0,64	0,00E+00
MITF	KIT	0,50	4,61E-06	0,55	0,00E+00
MITF	ETV1	0,57	1,08E-07	0,64	0,00E+00
MITF	MITF	1,00	0,00E+00	1,00	0,00E+00

Figure 1

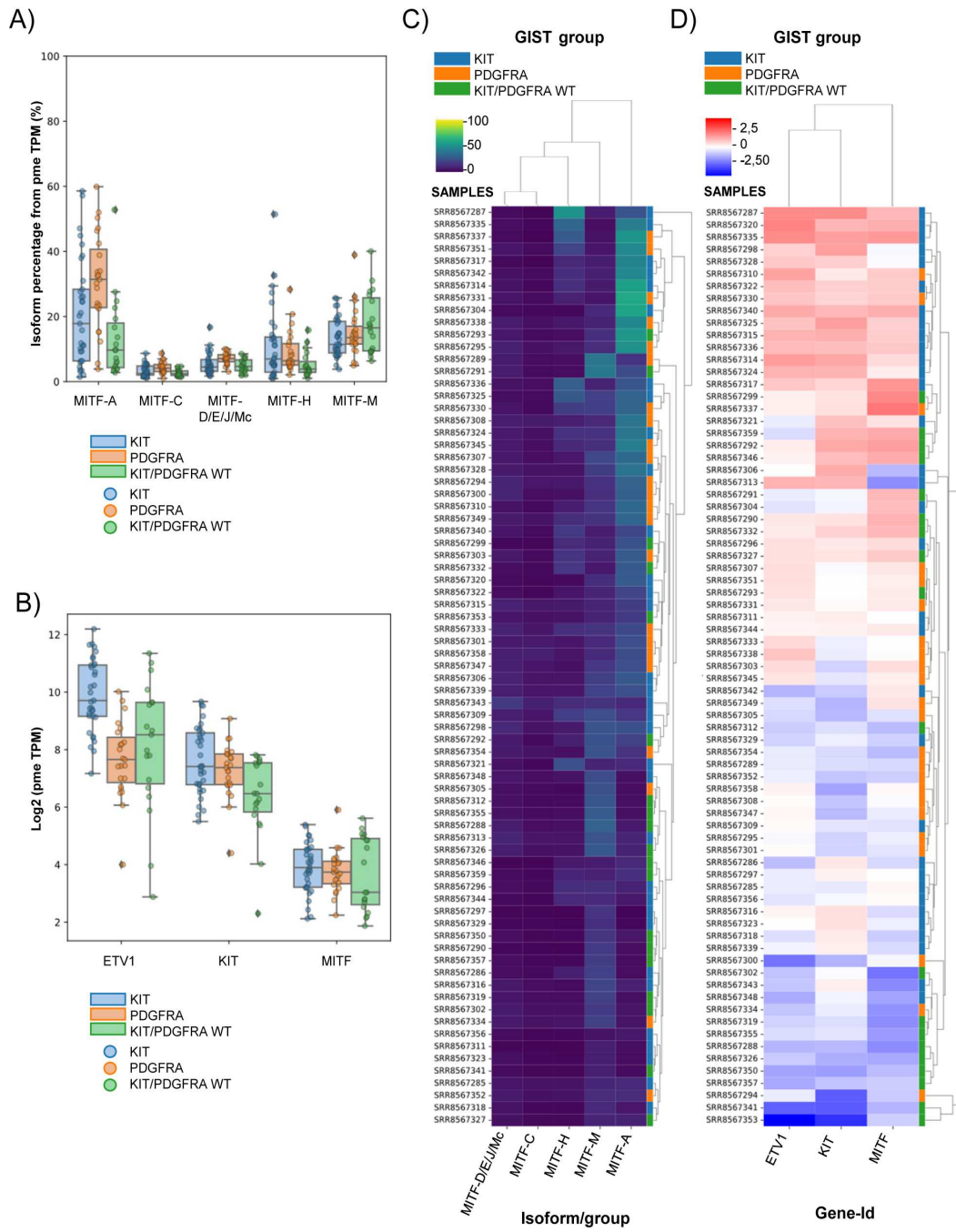


Figure 2

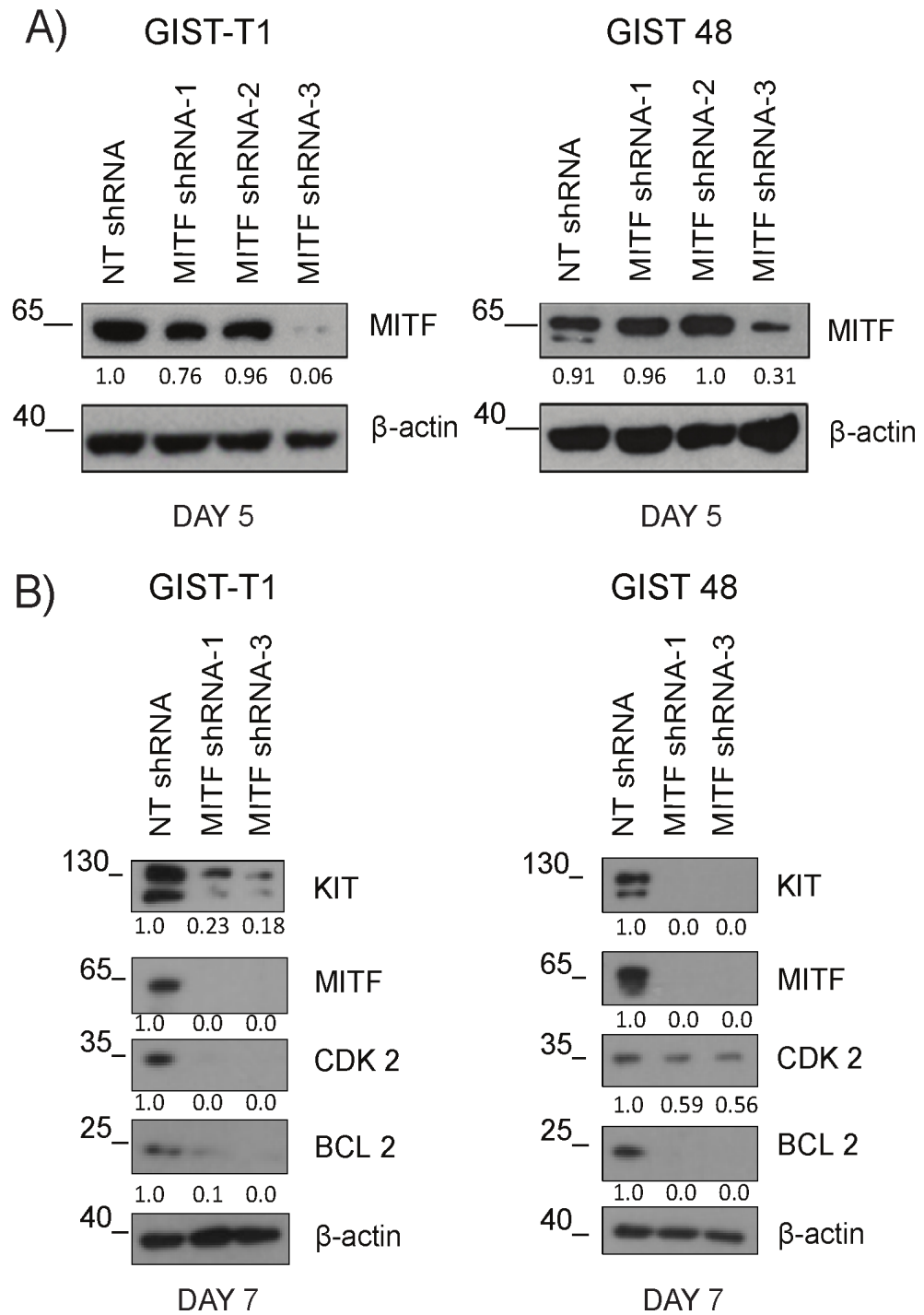


Figure 3

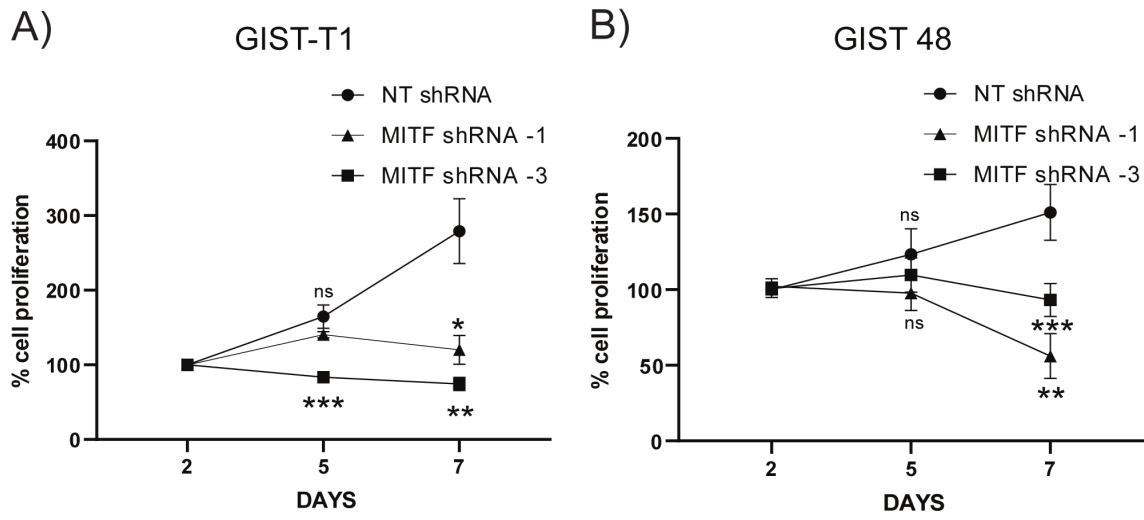


Figure 4

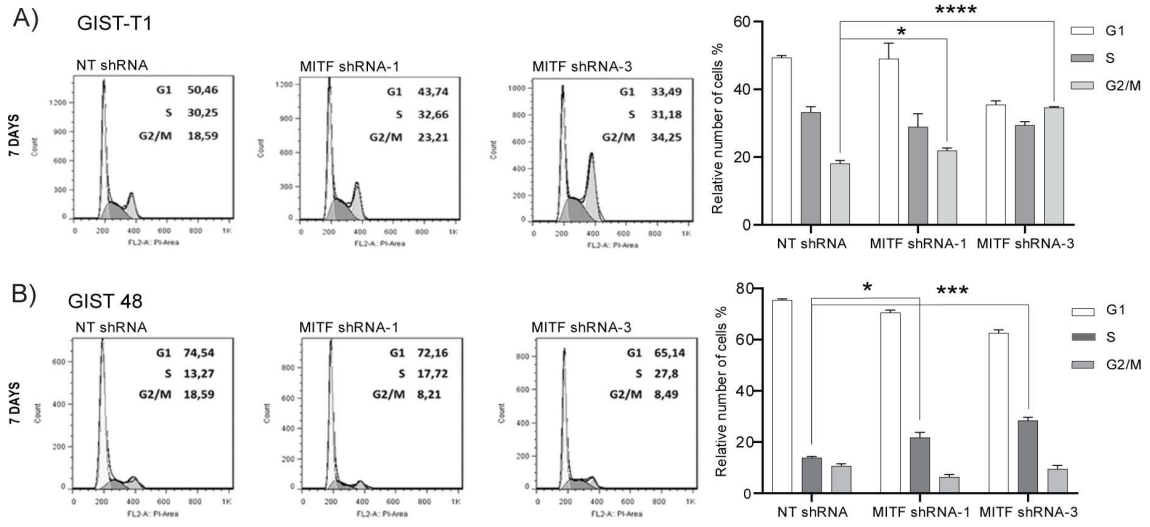


Figure 5

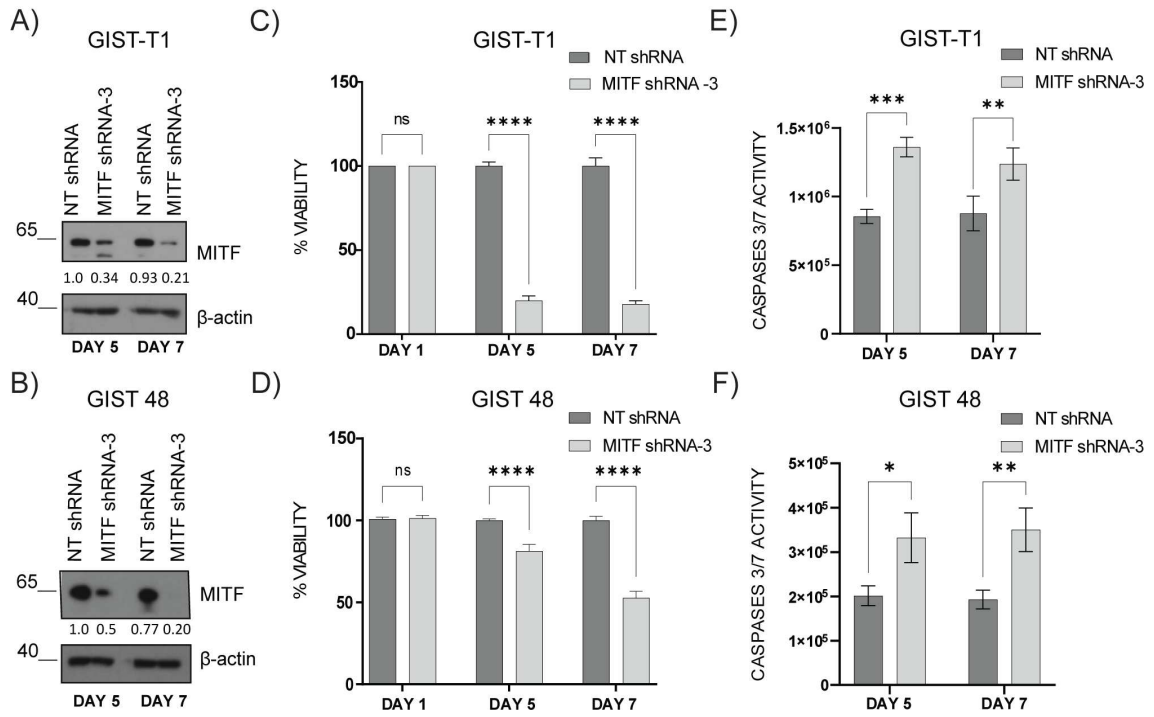


Figure 6

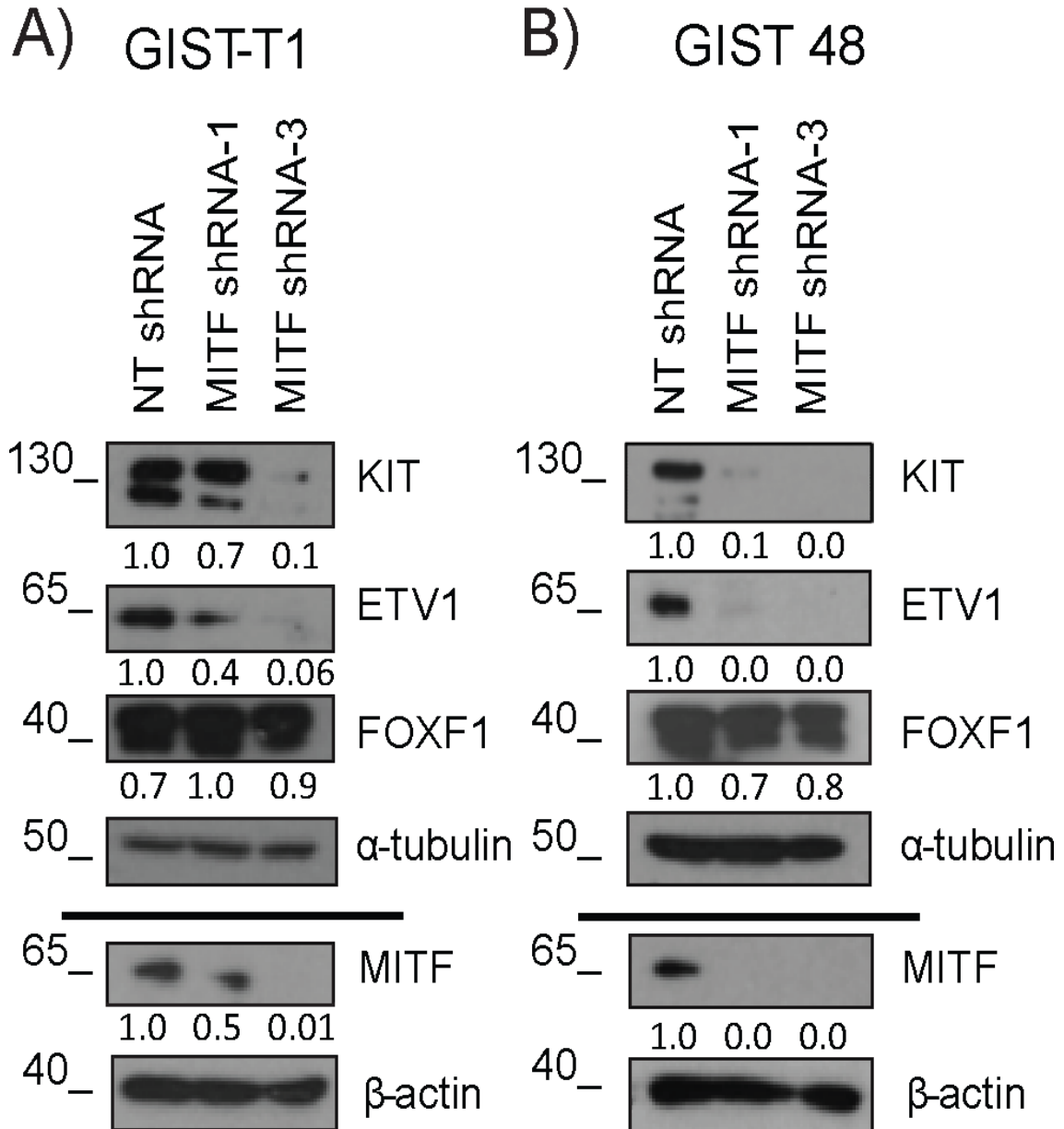


Figure 7

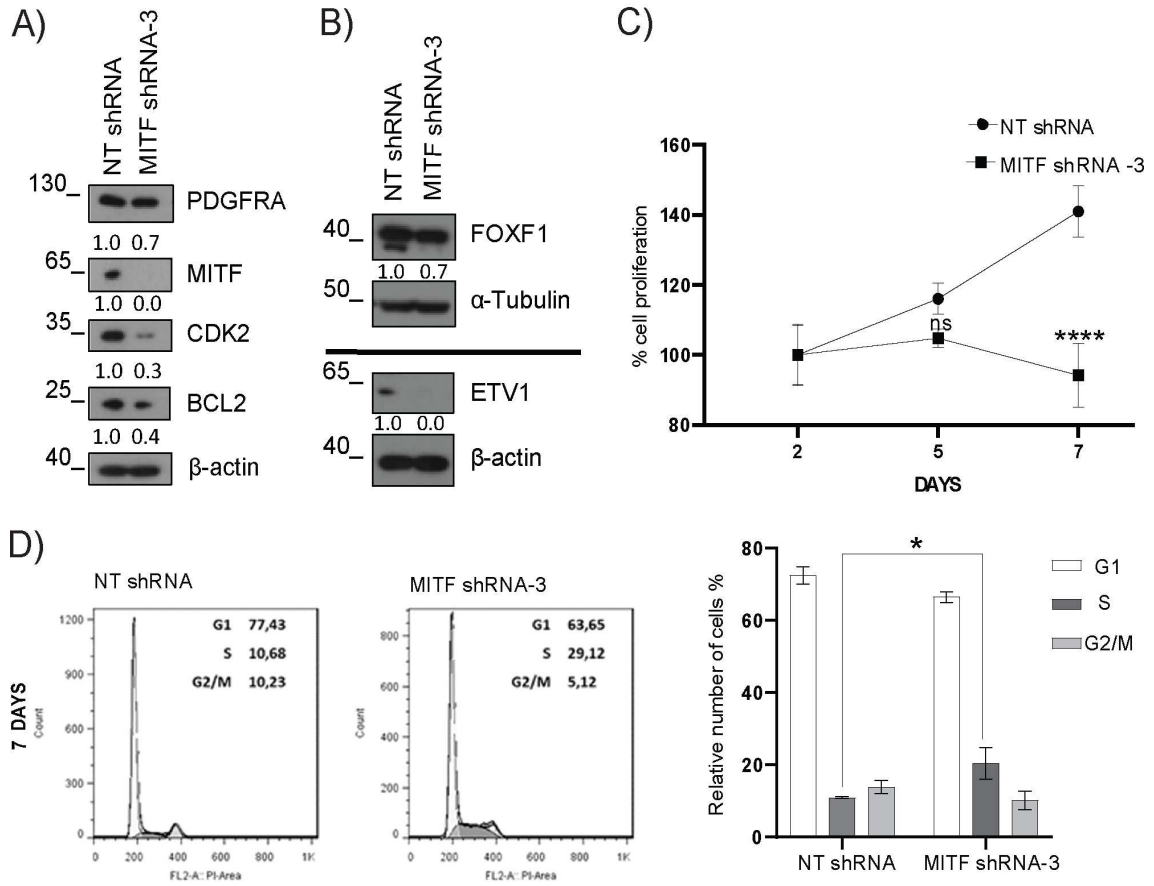


Figure 8

